

## Growth Mechanism of Benzene Clusters and Crystalline Benzene

BY SETSUKO OIKAWA, MINORU TSUDA, HIROMI KATO AND TADASHI URABE

Laboratory of Physical Chemistry, Pharmaceutical Sciences, Chiba University, Chiba 260, Japan

(Received 24 January 1985; accepted 1 July 1985)

### Abstract

The structure of a benzene cluster is determined from a dimer up to an assembly of 42 molecules by theoretical calculations utilizing the atomic pair potential function (*R*-1-4-6-12 type) proposed by Fraga (*J. Comput. Chem.* (1982), **3**, 329-334]. The conclusions are as follows: (*a*) the fundamental unit of cluster structure is the *T*-shaped pair of benzene molecules; (*b*) the smallest stable cluster structure, the nucleus of crystal growth, is the hexamer; (*c*) the monolayer cluster is produced by subsequently surrounding the hexamer with a *T*-shaped pair made with an additional benzene molecule; (*d*) the island grown on the monolayer surface proceeds in such a way that an incoming molecule stands almost perpendicularly at the center of a tetrameric part of the monolayer, subsequently surrounding the first member of the island; (*e*) the structure of the benzene crystal is reproduced at the center of the large three-dimensionally symmetrical cluster.

### Introduction

Recently, several spectroscopic (Duncan, Dietz, Liverman & Smalley, 1981; Hopkins, Powers & Smalley, 1981; Langridge-Smith, Brumbaugh, Haynam & Levy, 1981) and electron diffraction studies (Heenan, Valente & Bartell, 1982) have been carried out on the structures of small benzene clusters formed in a monoatomic carrier gas. Benzene dimers, trimers, tetramers *etc.* were observed in these spectra, but their geometrical configurations still remain obscure. Williams (1980) has calculated benzene-cluster structures from a dimer to a pentadecamer with his non-bonded pair potential function, but the structures estimated were very different from the arrangements found in benzene crystals (Cox, Cruickshank & Smith, 1958; Bacon, Curry & Wilson, 1964; Narten, 1967). Van de Waal (1981) also calculated the structure of benzene clusters but no good result was obtained.

In this paper, the structures of benzene clusters from a dimer to an assembly of 42 molecules are calculated by utilizing the atomic pair potential function developed by Fraga. At variance with the Williams's and van de Waal's results, cluster conformations obtained by the present method reflect well the

observed crystal data. So the present calculation may be expected to elucidate in more detail the mechanism of nucleation and growth of molecular crystals.

### Method of calculation

*Formulation of molecular interaction energy calculations utilizing the atomic pair potential function*

Although *a priori* quantum-mechanical calculations for molecular assemblies may be desirable for an accurate elucidation of nucleation and growth of molecular crystals, they are still prohibitive because of the economical and computational limits. There are various kinds of semiempirical calculations that have been used for the problem by several authors (*e.g.* Clementi, 1980). Fraga (1982) approximated the interaction energy between two molecules, *A* and *B*, by

$$E_{AB} = \sum_a^{\text{on } A} \sum_b^{\text{on } B} [C(1)_{ab}/R_{ab} + C(4)_{ab}/R_{ab}^4 + C(6)_{ab}/R_{ab}^6 + C(12)_{ab}/R_{ab}^{12}], \quad (1)$$

where  $R_{ab}$  is the distance between atoms *a* and *b* belonging to molecules *A* and *B*, respectively, and the summations extend to all the couples of atoms in the two molecules. The expansion coefficients  $C(1)_{ab}$ ,  $C(4)_{ab}$ ,  $C(6)_{ab}$  and  $C(12)_{ab}$  are determined for each pair of atomic species [*e.g.*  $C(1)_{\text{H-H}}$ ,  $C(1)_{\text{H-C(ring)}}$  *etc.*] in such a way that (1) reproduces the interaction energies of pairs of molecules of various kinds that have been obtained by *ab initio* calculations (Clementi, Cavallone & Scordamaglia, 1977). The coefficients given by Fraga (1982) have been used in this paper.

The total interaction energy of a cluster containing *N* molecules is given by

$$E_{\text{total}}(N) = (1/2) \sum_{A \neq B} \sum E_{AB}, \quad (2)$$

where the summations are extended to all the molecules contained in the cluster except the case of  $A = B$ .

### Determination of cluster structure

The geometry of the benzene molecule has been fully optimized by *ab initio* calculation in this research

Table 1. *The atomic configuration of the benzene molecule ( $\text{\AA}$ )*

The coordinates are the result of a fully optimized determination by *ab initio* calculations with a 3-21G basis set.

|      | x        | y        | z       |
|------|----------|----------|---------|
| C(1) | 0.69225  | 1.19901  | 0.00000 |
| C(2) | -0.69225 | 1.19901  | 0.00000 |
| C(3) | -1.38450 | 0.00000  | 0.00000 |
| C(4) | -0.69225 | -1.19901 | 0.00000 |
| C(5) | 0.69225  | -1.19901 | 0.00000 |
| C(6) | 1.38450  | 0.00000  | 0.00000 |
| H(1) | 1.22830  | 2.12748  | 0.00000 |
| H(2) | -1.22830 | 2.12748  | 0.00000 |
| H(3) | -2.45660 | 0.00000  | 0.00000 |
| H(4) | -1.22830 | -2.12748 | 0.00000 |
| H(5) | 1.22830  | -2.12748 | 0.00000 |
| H(6) | 2.45660  | 0.00000  | 0.00000 |

with the 3-21G basis set (Binkley, Pople & Hehre, 1980). The determined molecular structure (Table 1) was fixed in all the subsequent calculations on cluster structures, which were performed by minimizing the total interaction energy obtained by (2). Equation (2) is a function of  $6N$  variables, which determine the structure of a cluster, *i.e.*

$$E_{\text{total}}(N) = F(X_1, Y_1, Z_1, \alpha_1, \beta_1, \gamma_1, X_2, Y_2, Z_2, \alpha_2, \beta_2, \gamma_2, \dots, X_N, Y_N, Z_N, \alpha_N, \beta_N, \gamma_N, \dots), \quad (3)$$

where  $N$  is the number of molecules contained in a cluster,  $X_i, Y_i, Z_i$  are the Cartesian coordinates of the center of mass of the  $i$ th molecule and  $\alpha_i, \beta_i, \gamma_i$  are the rotation angles around the three orthogonal axes that cross at the point  $(X_i, Y_i, Z_i)$  and are parallel to the Cartesian coordinates for the central molecule of the cluster as shown in Fig. 1. Rotation operation is carried out in the order  $x, y, z$ . Once each of the  $6N$  variables is given,  $E_{\text{total}}(N)$  is calculated by (2) through (1). The minimization of the total interaction energy,  $E_{\text{total}}(N)$ , is performed by determining the steepest descent path from any point to the minimum point on the  $6N$ -dimensional interaction-energy hypersurface. Since the steepest descent finds the nearest minimum on the energy hypersurface, which is sometimes a local minimum, the most stable structure of the cluster was determined as the absolute minimum by calculating all the possible configurations of the cluster.

In practice, two kinds of gradients of  $E_{\text{total}}(N)$  with respect to each of the  $3N$  variables, the  $3N$  coordinates of the center of mass ( $X_i, Y_i, Z_i, i = 1, 2, \dots, N$ ) and the  $3N$  rotational angles ( $\alpha_i, \beta_i, \gamma_i, i = 1, 2, \dots, N$ ), are evaluated separately and the minimum point is searched step by step until each of the gradients converges within each of the threshold values ( $0.01 \text{ kJ mol}^{-1} \text{\AA}^{-1}$  and  $0.05 \text{ kJ mol}^{-1} \text{ degree}^{-1}$ ). The original Fortran program written by Fraga (1983) for minimizing the interaction energy

using six variables was extended and generalized to a program for the  $6N$ -dimensional interaction energy hypersurface by the present authors following the logic stated here.

### Analysis of stabilization energy in the cluster growth

The total interaction energy, the stabilization energy following cluster growth (abbreviated as 'cluster energy' below), was analyzed in this paper by  $E_{\text{pair}}(N)$ , which is defined by

$$E_{\text{pair}}(N) = [E_{\text{total}}(N) - E_{\text{total}}(N-1)] \times [m(N) - m(N-1)]^{-1}, \quad (4)$$

where  $E_{\text{total}}(N)$  is the total interaction energy of a cluster containing  $N$  molecules and  $m(N)$  is the number of  $T$ -shaped pairs in the cluster.  $E_{\text{pair}}(N)$  is the increment of the stabilization energy contributed by each of the  $T$ -shaped pairs formed in the cluster.  $E_{\text{pair}}(N)$  has a similar value in all of the clusters except for the tetramer and the hexamer as shown in Table 2. An extraordinary stabilization occurs in the formations of the tetramer and the hexamer, which are the fundamental structure of the benzene cluster. The value of  $E_{\text{pair}}(N)$  converges to a constant value,  $-6.9 \text{ kJ mol}^{-1}$ . A smaller value of  $E_{\text{pair}}(N)$  for small clusters means that these infant clusters are unstable.

## Results and discussion

### Monolayer growth of benzene cluster

First of all, the structure of the dimer, the most basic cluster, was determined as the absolute minimum on the  $6N$ -dimensional interaction energy

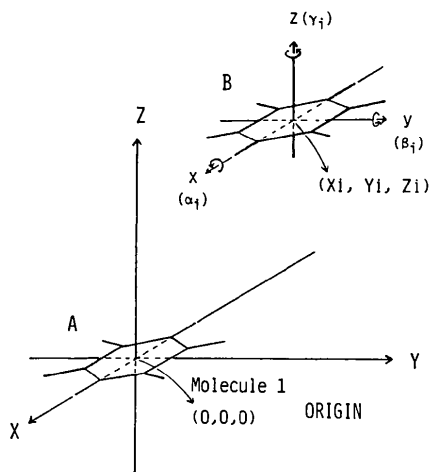


Fig. 1. An example of the geometrical configuration used for the calculation of  $E_{\text{total}}(N)$  (the case of two molecules at the start of calculation).

Table 2. Cluster energies and their analyses in monolayer cluster formation

| Molecules in cluster | $E_{\text{total}}(N)^*$<br>(kJ mol <sup>-1</sup> ) | $E_{\text{pair}}(N)^\dagger$<br>(kJ mol <sup>-1</sup> ) |
|----------------------|----------------------------------------------------|---------------------------------------------------------|
| 2 (1)‡               | -6.05                                              | -6.05                                                   |
| 3 (3)                | -17.12                                             | -5.54                                                   |
| 4 (4)                | -26.42                                             | -9.30                                                   |
| 5 (6)                | -36.30                                             | -4.94                                                   |
| 6 (7)                | -46.42                                             | -10.12                                                  |
| 7 (8)                | -54.69                                             | -8.27                                                   |
| 8 (10)               | -67.70                                             | -6.51                                                   |
| 9 (12)               | -80.43                                             | -6.37                                                   |
| 16 (24)              | -162.85                                            | -6.87 (av.)                                             |
| 36 (60)              | -412.81                                            | -6.94 (av.)                                             |

\* Total interaction energy (cluster energy).

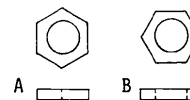
† Increment of cluster energy per *T*-shaped pair added.

‡ Numerals in parentheses are the number of *T*-shaped pairs in the cluster.

hypersurface (Fig. 2). Then the most stable structures of monolayer benzene clusters from the trimer up to the big cluster containing 36 molecules were determined step by step in the same way. Cluster structures determined by full optimization are shown in Figs. 2-11 by the one-point perspective where the position of the observer is along the *Y* axis (see Fig. 1). The geometrical parameters expressed by ( $X_i$ ,  $Y_i$ ,  $Z_i$ ,  $\alpha_i$ ,  $\beta_i$ ,  $\gamma_i$ ) are collected in Table 3. The total interaction energies are summarized in Table 2 as the cluster energy.

**Dimer:** A benzene dimer has  $C_{2v}$  symmetry as shown in Fig. 2, where two benzene rings are oriented like the letter *T* (*T* shaped). This result is in accordance with the observation by Janda, Hemminger, Winn, Novick, Harris & Klemperer (1975). They found by molecular beam analysis that the benzene dimer has an electric dipole moment or is a polar molecule, and concluded that a benzene dimer does not have a parallel structure. In the present research, the parallel orientation has no minimum on the 6*N*-dimensional interaction-energy hypersurface. Although there are two possibilities for the orientation of a benzene dimer (*A* and *B* below), type *A* (cluster energy  $-6.05$  kJ mol<sup>-1</sup>) is more stable than

type *B* (cluster energy  $-4.98$  kJ mol<sup>-1</sup>). This is in accordance with Fraga's (1982) result.



Hereafter all the calculations are carried out on type *A*. The intermolecular distance between molecular centers is  $5.497$  Å in the dimer and it becomes smaller following the growth of the cluster as summarized in Table 6.

**Trimer:** There are four ways of trimer formation as shown in Fig. 2. The most stable structure of the trimer (Fig. 3*a*), where each benzene molecule is placed on one side of a regular triangle, is obtained by a benzene molecule approaching the dimer from directions (1) and (2) in Fig. 2. The cluster energy of the trimer is  $-17.12$  kJ mol<sup>-1</sup>. Remarkable stabilization of the trimer compared with the dimer (cluster energy  $-6.05$  kJ mol<sup>-1</sup>) originates from the three *T*-shaped interaction sites, because the increment per *T*-shaped pair,  $E_{\text{pair}}(3)$ , is smaller than  $E_{\text{pair}}(2)$ . Benzene molecules approaching from (3) and (4) in Fig. 2 give two kinds of metastable trimer conformations shown in Figs. 3(*b*) and (*c*), with cluster energies  $-11.82$  and  $-11.99$  kJ mol<sup>-1</sup>, respectively.

**Tetramer:** There are three ways for a benzene molecule to approach the most stable trimer. The most stable tetramer (Fig. 4*a*) is produced in every case. Each benzene ring is placed on one side of the regular square of the tetramer. This structure also looks like two *T* bars, one inverted, coupled side by side. The cluster energy is  $-26.42$  kJ mol<sup>-1</sup>. The large  $E_{\text{pair}}(4)$  value of  $-9.30$  kJ mol<sup>-1</sup> shows that the tetramer formation largely stabilizes the cluster system. One finds the same regular square structure on the (002) plane in the unit cell of the benzene crystal

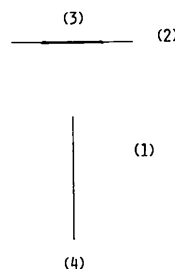


Fig. 2. Dimer. An approach of a benzene molecule from the directions (1) and (2) produces the trimer in Fig. 3(*a*). Other approaches from (3) and (4) produce metastable trimers in Figs. 3(*b*) and (*c*), respectively.

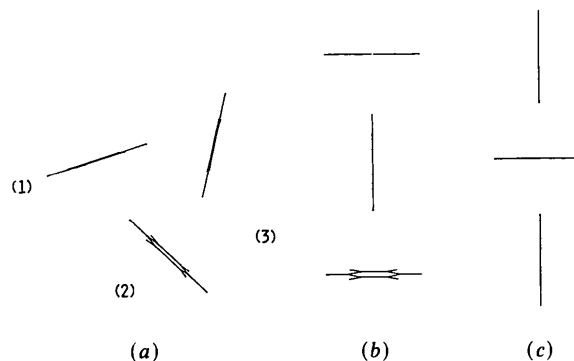


Fig. 3. (*a*) The most stable trimer. All approaches from (1), (2) and (3) produce the most stable tetramer of Fig. 4(*a*). (*b*) A metastable trimer, which produces the metastable tetramer of Fig. 4(*b*). (*c*) Another metastable trimer, which also produces the metastable tetramer of Fig. 4(*b*).

Table 3. *Molecular configurations of monolayer clusters* ( $\text{\AA}$ ,  $^\circ$ )

$X_i, Y_i, Z_i$  are Cartesian coordinates of the  $i$ th molecular center and  $\alpha_i, \beta_i, \gamma_i$  are rotational angles around the  $x, y, z$  axes (see Fig. 1). Molecule 1 is placed at the origin and not rotated ( $X_1, Y_1, Z_1, \alpha_1, \beta_1, \gamma_1$  are all zero).

| Cluster  | $i$ | $X_i$   | $Y_i$  | $Z_i$   | $\alpha_i$ | $\beta_i$ | $\gamma_i$ |
|----------|-----|---------|--------|---------|------------|-----------|------------|
| Dimer    | 2   | 0.0000  | 0.0000 | 5.4966  | 0.0000     | 90.0000   | 0.0000     |
|          | 2   | 0.6132  | 0.0000 | -5.5078 | 0.0000     | 60.0879   | 0.0000     |
| Trimer   | 3   | 5.0729  | 0.0000 | -2.2181 | 0.0000     | 299.8986  | 0.0000     |
|          | 2   | -5.4726 | 0.0000 | -0.0038 | 0.0000     | -90.0000  | 0.0000     |
| Tetramer | 3   | -5.4688 | 0.0000 | -5.4764 | 0.0000     | 0.0000    | 0.0000     |
|          | 4   | 0.0038  | 0.0000 | -5.4726 | 0.0000     | -90.0000  | 0.0000     |
|          | 2   | 0.7993  | 0.0000 | 5.4781  | 0.0000     | 100.1706  | 0.0000     |
| Pentamer | 3   | 5.3610  | 0.0000 | -0.5279 | 0.0000     | 285.2510  | 0.0000     |
|          | 4   | 6.2650  | 0.0000 | 4.8646  | 0.0000     | 4.0478    | 0.0000     |
|          | 5   | 2.4753  | 0.0000 | -5.1928 | 0.0000     | 56.1094   | 0.0000     |
| Hexamer  | 2   | 0.0236  | 0.0000 | 5.4782  | 0.0000     | 88.6500   | 0.0000     |
|          | 3   | 5.4983  | 0.0000 | 5.4810  | 0.0000     | -0.5338   | 0.0000     |
|          | 4   | 5.4430  | 0.0000 | 0.0000  | 0.0000     | 89.9969   | 0.0000     |
|          | 5   | 5.4983  | 0.0000 | -5.4810 | 0.0000     | 0.5391    | 0.0000     |
|          | 6   | 0.0236  | 0.0000 | -5.4782 | 0.0000     | 91.3565   | 0.0000     |
| Heptamer | 2   | 0.1075  | 0.0000 | 5.5065  | 0.0000     | 89.0939   | 0.0000     |
|          | 3   | 5.5894  | 0.0000 | 5.4106  | 0.0000     | 2.8773    | 0.0000     |
|          | 4   | 5.4281  | 0.0000 | 0.0000  | 0.0000     | 89.9905   | 0.0000     |
|          | 5   | 5.5894  | 0.0000 | -5.4107 | 0.0000     | -2.8744   | 0.0000     |
|          | 6   | 0.1075  | 0.0000 | -5.5065 | 0.0000     | 90.9126   | 0.0000     |
|          | 7   | 10.9204 | 0.0000 | 0.0000  | 0.0000     | 0.0024    | 0.0000     |
|          | 2   | -0.0004 | 0.0000 | 5.4985  | 0.0000     | 90.5025   | 0.0000     |
| Octamer  | 3   | 5.4896  | 0.0000 | 5.5047  | 0.0000     | 2.3337    | 0.0000     |
|          | 4   | 5.4349  | 0.0000 | 0.0744  | 0.0000     | 93.0750   | 0.0000     |
|          | 5   | 5.6194  | 0.0000 | -5.3281 | 0.0000     | -2.4744   | 0.0000     |
|          | 6   | 0.1432  | 0.0000 | -5.4993 | 0.0000     | 92.9007   | 0.0000     |
|          | 7   | 10.8977 | 0.0000 | -0.1068 | 0.0000     | 2.6858    | 0.0000     |
|          | 8   | 10.9738 | 0.0000 | 5.3830  | 0.0000     | 97.8024   | 0.0000     |
|          | 2   | 0.0000  | 0.0000 | 5.4573  | 0.0000     | 89.9941   | 0.0000     |
|          | 3   | 5.4736  | 0.0000 | 5.4800  | 0.0000     | -1.7865   | 0.0000     |
| Nonamer  | 4   | 5.4562  | 0.0000 | 0.0000  | 0.0000     | 89.9955   | 0.0000     |
|          | 5   | 5.4736  | 0.0000 | -5.4800 | 0.0000     | 1.7716    | 0.0000     |
|          | 6   | 0.0000  | 0.0000 | -5.4573 | 0.0000     | 89.9941   | 0.0000     |
|          | 7   | -5.4736 | 0.0000 | -5.4800 | 0.0000     | -1.7865   | 0.0000     |
|          | 8   | -5.4562 | 0.0000 | 0.0000  | 0.0000     | 89.9955   | 0.0000     |
|          | 9   | -5.4736 | 0.0000 | 5.4800  | 0.0000     | 1.7716    | 0.0000     |

(Evans, 1964). However, the tetramer structure does not seem to be completely stable, since the regular square structure is destroyed by pentamer formation. From two other kinds of metastable trimers, only one other type of tetramer structure is formed as shown in Fig. 4(b). This is a metastable tetramer (cluster energy  $-24.69 \text{ kJ mol}^{-1}$ ) and its  $E_{\text{pair}}(4)$  value [ $-4.29$  or  $-4.23 \text{ kJ mol}^{-1}$  from the trimer in Figs. 3(b) or (c), respectively] is very small.

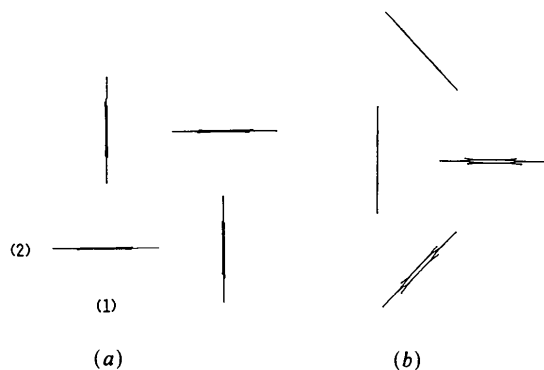


Fig. 4. (a) The most stable tetramer. Approaches from (1) and (2) produce the pentamer in Fig. 5. (b) A metastable tetramer.

**Pentamer:** It is interesting that the most stable and the metastable tetramers give the same pentamer structure, which is shown in Fig. 5 (cluster energy  $-36.30 \text{ kJ mol}^{-1}$ ). The regular square structure found in the most stable tetramer is destroyed and a lozenge-shaped structure is formed. The small  $E_{\text{pair}}(5)$  value ( $-4.94 \text{ kJ mol}^{-1}$ ) explains the poor contribution of the pentamer formation in the stabilization of the cluster system.

**Hexamer:** There are many ways for hexamer formation from the pentamer. Fig. 6 shows the most stable hexamer structure (cluster energy  $-46.42 \text{ kJ mol}^{-1}$ ), which is found in benzene crystals and also in the tetramer. The  $E_{\text{pair}}(6)$  value of the hexamer ( $-10.12 \text{ kJ mol}^{-1}$ ) is the largest in all the cluster formations examined in this research and this structure is maintained in all the bigger cluster structures. Therefore, the hexamer is obviously the stable nucleus produced first in the process of cluster growth.

**Heptamer:** Four kinds of stable heptamer were found as shown in Fig. 7, where the structure (a) gives the largest  $E_{\text{pair}}(7)$  value ( $-8.77 \text{ kJ mol}^{-1}$ ) among the four. Both of the structures [Figs. 7(a) cluster energy  $-54.69 \text{ kJ mol}^{-1}$  and (b) cluster energy  $-56.68 \text{ kJ mol}^{-1}$ ] are the nuclei of the totally sym-

metrical cluster growth observed in the octamer and nonamer formations. The heptamers of Figs. 7(c) and (d), whose cluster energies are  $-56.29$  and  $-56.71$  kJ mol $^{-1}$ , respectively, open other routes for cluster growth.

**Octamer:** The most stable structure for the octamer (cluster energy  $-67.70$  kJ mol $^{-1}$ ) shown in Fig. 8(a) is created from both heptamers of Figs. 7(a) and (b). It is interesting that the triangular structure found in Fig. 7(b) smoothly transforms to the regular square structure found in Fig. 8(a). The heptamer of Fig. 7(c) leads to the metastable octamer (cluster energy  $-66.50$  kJ mol $^{-1}$ ) shown in Fig. 8(b). The heptamer of Fig. 7(d) gives no stable octamer, and the triangular structure found in Fig. 7(d) needs an activation energy to recover the regular square structure found in a bigger cluster.

**Nonamer:** The most stable structure for the nonamer (cluster energy  $-80.43$  kJ mol $^{-1}$ ) shown in Fig. 9 is produced from the most stable octamer. The value of  $E_{\text{pair}}(N)$  converges to a constant value after hexamer formation as shown in Table 2.

**Hexadecamer and a large cluster of 36 molecules:** If the same mechanism continues for further cluster

growth, a hexadecamer and a larger cluster of 36 molecules are produced, whose structures are shown in Figs. 10(a) and (b), respectively. The average  $E_{\text{pair}}(N)$  values of these two clusters are substantially the same as the converged value (*ca*  $-6.94$  kJ mol $^{-1}$ ). This means that the basic part of the cluster structure is already completed by the step of hexamer forma-

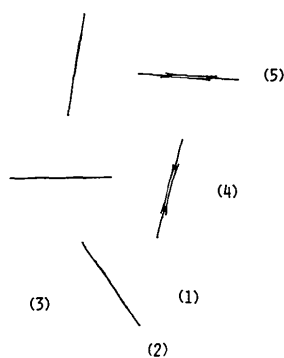


Fig. 5. Pentamer. Approaches from (1) and (3) produce the most stable hexamer in Fig. 6(a). Other approaches from (2), (4) and (5) give no stable hexamer, provided that no activation energy is given.

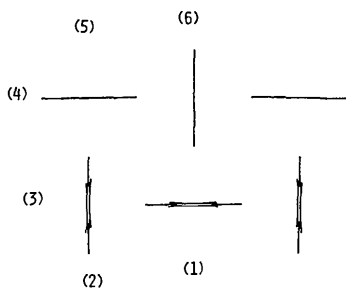


Fig. 6. Hexamer. Approaches from (1) and (2) produce the heptamers in Figs. 7(a) and (d), respectively. Approaches from (3) and (4) produce the heptamer of Fig. 7(c). Approaches from (5) and (6) produce the heptamer in Fig. 7(b).

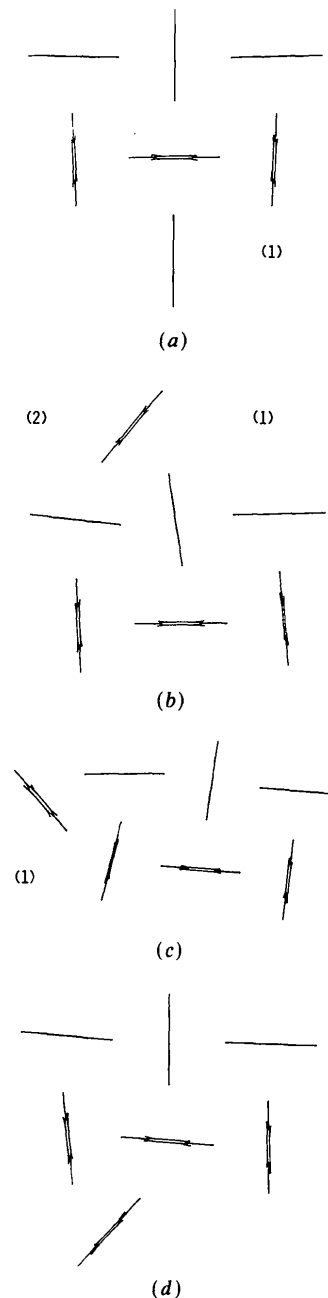


Fig. 7. Various structures of heptamers. Approaches to the heptamers of (a) and (b) produce the most stable octamer in Fig. 8(a). An approach to heptamer (c) produces the metastable octamer in Fig. 8(b). The heptamer (d) produces no stable octamer if no activation energy is given.

tion. Therefore, we can conclude again that a hexamer is the nucleus in the cluster (or crystal) growth.

The monolayer growth of benzene clusters is summarized as follows: (1) the fundamental unit of the benzene-cluster structure is the *T*-shaped structure; (2) the hexamer is the nucleus in cluster growth; (3) the cluster growth is performed by subsequently surrounding the hexamer as a nucleus with the fundamental *T*-shaped structure.

#### Growth of island cluster on monolayer surface

The second step in cluster formation is the growth in the vertical direction. In crystal growth, an island will first be produced on the surface of the crystal, although another possibility could be the growth on a screw dislocation. There is a critical condition to be satisfied for island formation. No molecule is stabilized on the monolayer when the monolayer cluster is small. When a benzene molecule approaches the center of a tetramer or a hexadecamer, no stabilized cluster is produced. However, when the structure of the hexadecamer was kept invariant, a benzene

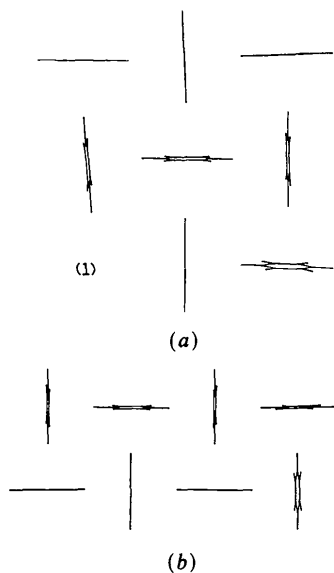


Fig. 8. (a) The most stable octamer. An approach from (1) produces a nonamer in Fig. 9. (b) A metastable octamer.

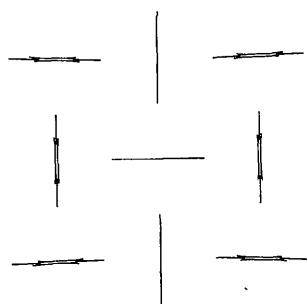


Fig. 9. The most stable nonamer.

Table 4. Cluster energies and their analyses in island formation on the monolayer consisting of 36 molecules

| Molecules in cluster    | $E_{\text{total}}(N)^*$<br>(kJ mol <sup>-1</sup> ) | $E'_{\text{total}}(N)^{\dagger}$<br>(kJ mol <sup>-1</sup> ) | $E_{\text{pair}}(N)^{\ddagger}$<br>(kJ mol <sup>-1</sup> ) |
|-------------------------|----------------------------------------------------|-------------------------------------------------------------|------------------------------------------------------------|
| 36                      | -412.81                                            |                                                             |                                                            |
| 36 + 1 (0) <sup>§</sup> | -420.83                                            | 0.0                                                         | 0.0                                                        |
| 36 + 2 (1)              | -431.97                                            | -3.12                                                       | -3.12                                                      |
| 36 + 3 (3)              | -443.14                                            | -6.27                                                       | -1.58                                                      |
| 36 + 4 (4)              | -461.90                                            | -17.01                                                      | -10.74                                                     |
| 36 + 5 (6)              | -474.72                                            | -21.81                                                      | -2.40                                                      |
| 36 + 6 (7)              | -493.08                                            | -32.15                                                      | -10.34                                                     |

\* Total interaction energy (cluster energy).

† Stabilization energy of the island cluster on the monolayer.

‡ Increment of the stabilization energy per *T*-shaped pair added.

§ Numerals in parentheses are the number of *T*-shaped pairs in the island cluster.

molecule stood alone at the center of the hexadecamer. 36 molecules form the minimum monolayer where the stabilization of the first monomer that produces the island takes place when all the molecules are free. In this case, the 20 molecules that make up the outermost part of the 36-molecule monolayer change their orientations following the stabilization of a benzene molecule at the center of the monolayer, but the 16 molecules of the inner part are substantially invariant. This shows that the monolayer at the crystal surface is substantially invariant when an island is formed on the surface.

The islands from a monomer to a hexamer produced on the monolayer consisting of 36 molecules are shown in Fig. 11, where the structure of 36

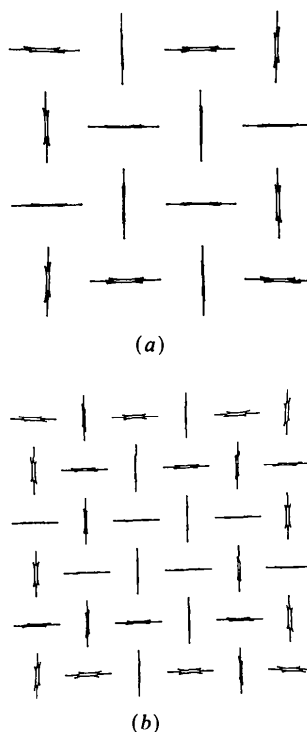


Fig. 10. (a) The most stable hexadecamer. (b) Monolayer cluster consisting of 36 molecules.

Table 5. *Molecular configurations of island clusters on the monolayer* ( $\text{\AA}, ^\circ$ )

$X_i, Y_i, Z_i$  are Cartesian coordinates of  $i$ th molecular center and  $\alpha_i, \beta_i, \gamma_i$  are rotational angles around the  $x, y, z$  axes (see Fig. 1).

| Island   | $i$ | $X_i$   | $Y_i$  | $Z_i$   | $\alpha_i$ | $\beta_i$ | $\gamma_i$ |
|----------|-----|---------|--------|---------|------------|-----------|------------|
| Monomer  | 1   | 0.0157  | 5.2823 | 0.0031  | 7.9828     | 13.6289   | 30.8228    |
| Dimer    | 1   | -0.0671 | 5.3185 | 0.0372  | 9.0212     | 12.7338   | 31.3493    |
|          | 2   | 0.1254  | 5.6202 | -5.4876 | 6.8695     | 77.4811   | 4.2957     |
| Trimer   | 1   | 0.2720  | 5.3001 | 0.0432  | 9.9410     | 10.4214   | 25.2523    |
|          | 2   | 0.7470  | 5.7097 | -5.5372 | 28.0700    | 77.9419   | 12.3491    |
|          | 3   | 5.4034  | 6.6274 | -1.2157 | 13.6731    | 289.0708  | -4.3145    |
| Tetramer | 1   | 0.1040  | 5.3026 | 0.0551  | 9.2198     | 9.6452    | 25.9635    |
|          | 2   | 0.1960  | 5.6852 | -5.4488 | 4.9927     | 80.7761   | 0.7720     |
|          | 3   | 5.4987  | 5.8007 | -0.1692 | -1.3065    | 80.7661   | -0.4279    |
|          | 4   | 5.6329  | 5.3698 | -5.6488 | 2.0689     | 12.3669   | 28.7327    |
| Pentamer | 1   | 0.0082  | 5.3131 | 0.0070  | 6.7748     | 11.0200   | 27.8412    |
|          | 2   | 0.0946  | 5.7097 | -5.4846 | 18.2486    | 78.9676   | 17.6229    |
|          | 3   | 5.3398  | 5.7473 | -0.0544 | -9.2508    | 79.2987   | -6.8010    |
|          | 4   | 5.4863  | 5.2912 | -5.5608 | 2.9064     | 12.8090   | 33.5188    |
|          | 5   | 0.1574  | 5.6592 | 5.4472  | -10.3560   | 79.7526   | -14.8471   |
| Hexamer  | 1   | 0.1106  | 5.3222 | 0.1213  | 9.6851     | 8.8573    | 26.3876    |
|          | 2   | 0.0630  | 5.8119 | -5.3535 | 11.5662    | 82.3443   | 9.5544     |
|          | 3   | 5.4826  | 5.7692 | -0.1018 | 0.6888     | 83.1785   | 1.5794     |
|          | 4   | 5.4402  | 5.2780 | -5.5925 | 2.4579     | 13.9782   | 34.1079    |
|          | 5   | 0.0401  | 5.5928 | 5.6231  | -21.1362   | 76.3220   | -25.7980   |
|          | 6   | 5.5462  | 5.3827 | 5.4022  | 6.6051     | 9.5490    | 28.4410    |

molecules has been kept invariant at the most stable one as the model of the crystal surface. The interaction energies and geometrical parameters are collected in Tables 4 and 5, respectively.

*Monomer stabilization on the monolayer:* The first benzene molecule that forms an island is stabilized on the center of the central tetramer of the monolayer consisting of 36 molecules as shown in Fig. 11(a). The molecule stands almost perpendicular to the monolayer (inclined  $10^\circ$ ). The monomer island grows to a dimer, a trimer, . . . , and a large island will be formed in the end on the monolayer as shown in Figs. 11(a)-(f).

The stabilization energy of the first monomer, which is the first member of the island produced on the monolayer of 36 molecules, is  $8.02 \text{ kJ mol}^{-1}$ . Since the island formation on the monolayer proceeds in the same way as for the first member, where the incoming molecule stands almost perpendicularly to the center of the tetramer part of the monolayer as shown in Fig. 11, the stabilization energy of  $8.02 \text{ kJ mol}^{-1}$  will increase constantly each time one molecule is added to the island growing on the surface of the monolayer cluster. Therefore,  $E_{\text{pair}}(N)$ , the increment of stabilization energy originating from one  $T$ -shaped pair formation, is calculated by (5) for the island growth instead of (4):

$$E_{\text{pair}}(N) = [E'_{\text{pair}}(N) - E'_{\text{pair}}(N-1)] \times [m(N) - m(N-1)]^{-1}, \quad (5)$$

where  $E'_{\text{pair}}(N) = [E_{\text{total}}(36+N) - E_{\text{total}}(36)] - 8.02N$ ,  $N$  is the number of molecules in the island and  $m(N)$  is the number of  $T$ -shaped pairs produced in the island. The values of  $E_{\text{pair}}(N)$  for island growth are collected in Table 4. The values are remarkably small compared with those obtained in the formation of a

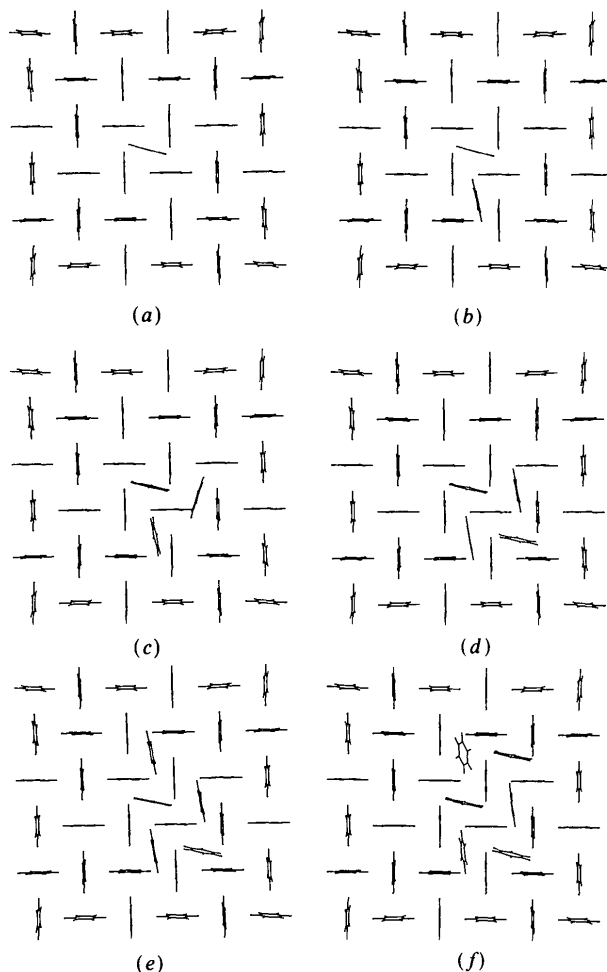


Fig. 11. (a) Monomer stabilized on the monolayer. (b) Dimer stabilized on the monolayer. (c) Trimer stabilized on the monolayer. (d) Tetramer stabilized on the monolayer. (e) Pentamer stabilized on the monolayer. (f) Hexamer stabilized on the monolayer.

monolayer cluster except for the tetramer and hexamer islands. This result strongly suggests that the tetramer and the hexamer are the nuclei in island growth on the monolayer surface. One should remember that the same result has been obtained in monolayer cluster formation.

#### Structure of the unit cell in benzene crystals

As shown above, there are two kinds of orientation of benzene dimer; *i.e.* type *A* and type *B*. Type *A* is the most stable orientation in all the clusters (see Figs. 2-11). On the other hand, only type-*B* orientation is observed in the benzene crystal. From what does this discrepancy originate?

Since a benzene crystal is formed from the unit cells of the lattice, which are themselves symmetrical, the most stable conformation of the three-dimensionally symmetrical cluster is expected to reflect the structure of the unit cells in the crystal. Structures of such symmetrical clusters containing 17 and 34 molecules determined under full geometry optimization are shown in Figs. 12 and 13. These clusters consist of three layers: four, nine and four molecules for the upper, middle and lower layers, respectively, in the heptamer, and nine, 16 and nine molecules in the cluster of 34 molecules. The same structure for the unit cell of the benzene crystal (Fig. 14) can be found at the center of both the symmetrical clusters in Figs. 12 and 13.

Figs. 12 and 13 clearly show that the orientation of the neighboring benzene dimer changes to type *B*

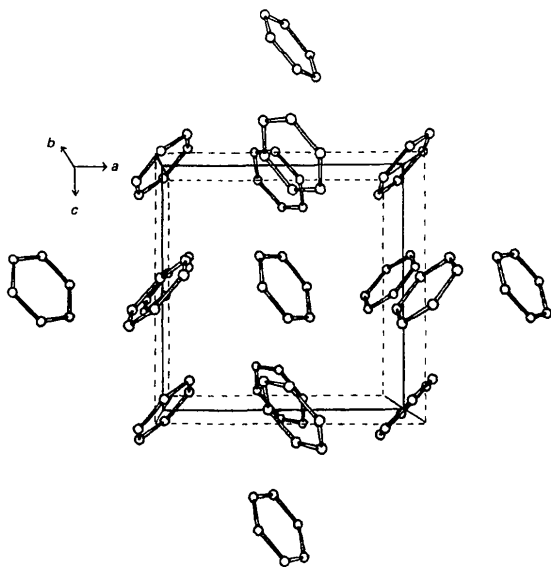


Fig. 12. An ORTEP (Johnson, 1965) view of the triple-layer cluster of 17 molecules, which consists of four, nine and four molecules for the upper, middle and lower layers, respectively. The upper and lower halves of the partial structure of the heptadecamer, which is within the frame, each correspond to half the unit cell of the benzene crystal. Only carbon atoms are drawn. The unit-cell edges are 8.585, 8.926 and 8.326 Å for *a*, *b* and *c*, respectively.

from type *A* at the center of these symmetrical clusters. Therefore, the conformational change from type *A* to type *B* may occur during crystal growth. Type *A* orientation is probably observed only in the infant clusters and the first layer of the crystal surface.

Intermolecular and interlayer distances of clusters are summarized in Table 6 together with data for a benzene crystal. As the cluster becomes larger, the intermolecular distance gradually converges to 5.459 Å or less. The interlayer distance converges to 5.0 Å or less. These values are in good agreement with those of the benzene crystal.

#### Concluding remarks

The structures of clusters from a dimer to a big assembly of 42 molecules were determined theoretically by using an atomic pair potential function which is based on the *ab initio* MO calculations. The results have given good information on the nucleation and growth of the monolayer cluster in space, the island formation and growth on the monolayer surface and

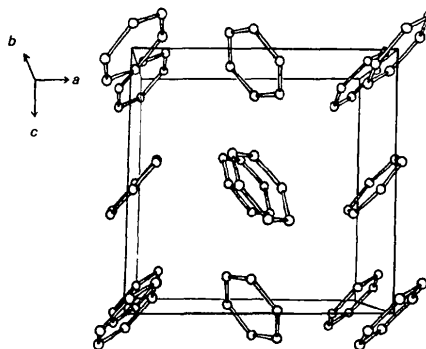


Fig. 13. An ORTEP (Johnson, 1965) view of the unit-cell structure found at the center of the triple-layer cluster containing 34 molecules, which consists of nine, 16 and nine molecules for the upper, middle and lower layers, respectively. Only carbon atoms are drawn. The unit-cell edges are 8.507, 9.017 and 8.017 Å for *a*, *b* and *c*, respectively.

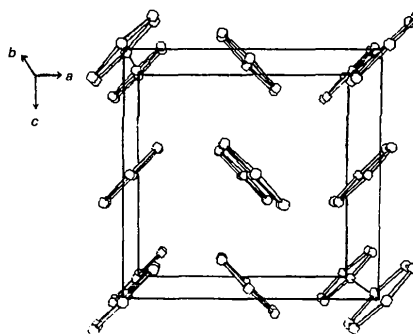


Fig. 14. An ORTEP (Johnson, 1965) view of the unit cell of the benzene crystal [solid at 270 K, Cox *et al.* (1958)]. Only carbon atoms are drawn. The unit-cell edges are 7.460, 9.666 and 7.034 Å for *a*, *b* and *c*, respectively.



Table 6. Intermolecular and interlayer distances of cluster

| Cluster      | Inter-molecular distance* (Å) | Cluster                   | Interlayer distance* (Å) |
|--------------|-------------------------------|---------------------------|--------------------------|
| (Monolayer)  |                               | (Island on the monolayer) |                          |
| Dimer        | 5.4967                        | Monomer                   | 5.2823                   |
| Tetramer     | 5.4726                        | Dimer                     | 5.4694                   |
| Nonamer      | 5.4668                        | Tetramer                  | 5.5396                   |
| Hexadecamer  | 5.4658                        | Hexamer                   | 5.5261                   |
| 36 molecules | 5.4586                        | (triple layer)            |                          |
|              |                               | Heptadecamer              | 4.4629                   |
| Exp.†        | 5.13                          | 34 molecules              | 4.4949                   |
|              |                               | Exp.†                     | 4.833                    |

\*Average value.

†Benzene crystal at 270 K (Cox *et al.*, 1958).

the crystal formation at the center of the three-dimensionally symmetrical cluster. A more realistic model for the unit cell of a benzene crystal would be obtained if one were to consider a cluster consisting of 168 molecules with a pentalayer structure: *i.e.* 16, 36, 64, 36 and 16 molecules for the top, second, third (middle), fourth and bottom layers, respectively, because this is the smallest cluster in which the unit cell of a benzene crystal is reproduced at the center with none of the members of the unit cell at the surface of the cluster. Unfortunately, such a huge calculation has not been performed because of the economical and computational limits, although quantitative information is expected if it could be done.

The authors are indebted to Professor S. Fraga for an early release of his program, *SOMAR* (Simulation of molecular associations and chemical reactions). The computations were carried out at the Computer

Center, the University of Tokyo, and the Computer Center, Chiba University. The authors thank the Computer Center, Institute for Molecular Science, Okazaki, for the use of the Hitac M-200H computer for a small part of the calculation. This work is supported in part by Grant in Aid for Scientific Research No. 59103011 from the Ministry of Education, Science and Culture.

## References

- BACON, G. E., CURRY, N. A. & WILSON, S. A. (1964). *Proc. R. Soc. London Ser. A*, **279**, 98–110.
- BINKLEY, J. S., POPE, J. A. & HEHRE, W. J. (1980). *J. Am. Chem. Soc.* **102**, 939–947.
- CLEMENTI, E. (1980). *Computational Aspects for Large Chemical Systems*. Berlin, Heidelberg: Springer Verlag.
- CLEMENTI, E., CAVALLONE, F. & SCORDAMAGLIA, R. (1977). *J. Am. Chem. Soc.* **99**, 5531–5557.
- COX, F. G., CRUICKSHANK, D. W. J. & SMITH, J. S. S. (1958). *Proc. R. Soc. London Ser. A*, **247**, 1.
- DUNCAN, M. A., DIETZ, T. G., LIVERMAN, M. G. & SMALLEY, R. E. (1981). *J. Phys. Chem.* **85**, 7.
- EVANS, R. C. (1964). *An Introduction to Crystal Chemistry*, 2nd ed., p. 385. Cambridge Univ. Press.
- FRAGA, S. (1982). *J. Comput. Chem.* **3**, 329–334.
- FRAGA, S. (1983). *Comput. Phys. Commun.* **29**, 351–359.
- HEENAN, R. K., VALENTE, E. J. & BARTELL, L. S. (1982). *J. Chem. Phys.* **78**, 243–248.
- HOPKINS, J. B., POWERS, D. E. & SMALLEY, R. E. (1981). *J. Phys. Chem.* **85**, 3739–3742.
- JANDA, K. C., HEMMINGER, J. C., WINN, J. S., NOVICK, S. E., HARRIS, S. J. & KLEMPERER, W. (1975). *J. Chem. Phys.* **63**, 1419–1421.
- JOHNSON, C. K. (1965). *ORTEP*. Report ORNL-3794. Oak Ridge National Laboratory, Tennessee.
- LANGRIDGE-SMITH, P. R. R., BRUMBAUGH, D. V., HAYNAM, C. A. & LEVY, D. H. (1981). *J. Phys. Chem.* **85**, 3742–3746.
- NARTEN, A. H. (1967). *J. Chem. Phys.* **48**, 1630.
- WAAL, B. W. VAN DE (1981). *Acta Cryst.* **A37**, 762–764.
- WILLIAMS, D. E. (1980). *Acta Cryst.* **A36**, 715–723.

*Acta Cryst.* (1985). **B41**, 445–452

## A New Type of $\sigma$ -Sulfurane with a Transannular S...N Bond: Structures of S-Substituted N-Methyl-6,7-dihydro-5H,12H<sup>+</sup>-dibenzo[b,g][1,5]thiazocinium Salts and N-Methyl-6,7-dihydro-5H-dibenzo[b,g][1,5]thiazocine S-Oxide

BY FUJIKO IWASAKI\*

Department of Materials Science, The University of Electro-Communications, Chofu-shi, Tokyo 182, Japan

AND KIN-YA AKIBA

Department of Chemistry, Faculty of Science, Hiroshima University, Hiroshima 730, Japan

(Received 1 February 1985; accepted 22 April 1985)

### Abstract

5H,12H<sup>+</sup>-Dibenzo[b,g][1,5]thiazocinium hexafluorophosphate (I), 12-methoxy-6-methyl-6,7-dihydro-5H,12H<sup>+</sup>-dibenzo[b,g][1,5]thiazocinium hexachloro-

antimonate (II), 6,12-dimethyl-6,7-dihydro-5H,12H<sup>+</sup>-dibenzo[b,g][1,5]thiazocinium hexafluorophosphate (III) and 6-methyl-6,7-dihydro-5H-dibenzo[b,g][1,5]thiazocine S-oxide (IV) were determined by the X-ray method. Crystal data: (I) C<sub>15</sub>H<sub>15</sub>CIN<sup>+</sup>.PF<sub>6</sub><sup>-</sup>, *M<sub>r</sub>* = 421.77, orthorhombic, *Pbca*,

\* To whom all correspondence should be addressed.